PCCP

PAPER

View Article Online
View Journal | View Issue

Cite this: *Phys. Chem. Chem. Phys.*, 2025, **27**, 16172

A study of the atmospherically relevant reaction between dimethyl sulphide (DMS) and Cl_2 in the absence and presence of water using electronic structure methods†

Lydia Rhyman, *[ab] Edmond P. F. Lee,[c] Ponnadurai Ramasami *[ab] and John M. Dyke *[c]

The thermodynamics and mechanisms of the atmospherically relevant reaction between dimethyl sulphide (DMS) and molecular chlorine (Cl_2) were investigated in the absence and presence of a single water molecule, using electronic structure methods. Stationary points on the reaction surfaces were located using density functional theory (DFT) with the M06-2X functional and aug-cc-pVTZ (aVTZ) basis sets. Then single point energy calculations were carried out using the UM06-2X/aVTZ optimised stationary point geometries, with aug-cc-pVnZ basis sets (n = T and Q), using the domain-based local pair natural orbitals coupled cluster [DLPNO-UCCSD(T)] method, to give DLPNO-CCSD(T)/CBS//M06-2X/aVTZ relative energies. The reaction can proceed in three ways depending on the initial van der Waals complex formed *i.e. via* DMS + Cl_2·H_2O, DMS·H_2O + Cl_2, or DMS·Cl_2 + H_2O. It was found that based on computed equilibrium constants for complex formation and estimated initial concentrations of DMS, Cl_2 and H_2O in the atmosphere that [DMS·H_2O] and [Cl_2·H_2O] are likely to be much greater than [DMS·Cl_2] under atmospheric conditions. It was found that both with and without water the reaction can proceed by two pathways (i) formation of the products CH_3SCH_2Cl + HCl + (H_2O) *via* a covalently bound intermediate $(CH_3)_2SCl_2(H_2O)$ and (ii) formation of the products *via* a *cis*-CH_3SClCH_2:HCl (H_2O) intermediate, where (H_2O) applies to the with-water case. Although the pathways and mechanisms are similar in the without- and with-water cases, the relative energies of the transition states are significantly lower and the potential energy diagram is much more complex in the with-water case. However, under tropospheric conditions the overall DMS + Cl_2 rate coefficient is unlikely to be affected by the presence of water as the concentrations of DMS·H_2O and Cl_2·H_2O are estimated to be much lower than the concentrations of DMS, Cl_2 and H_2O. This work extends our earlier study of the reaction of DMS with atomic chlorine (Cl) with and without water (L. Rhyman *et al.*, *Phys. Chem. Chem. Phys.* 2023, **25**, 4780–4793).

Received 2nd June 2025,
Accepted 10th July 2025

DOI: 10.1039/d5cp02065d

rsc.li/pccp

1. Introduction

In this work the atmospherically important reaction between molecular chlorine and dimethyl sulphide (DMS), reaction (1) is studied,

$$CH_3SCH_3 + Cl_2 \rightarrow CH_3SCH_2 + HCl \qquad (1)$$

in the absence and presence of a single water molecule.

The sulphur cycle in the earth's atmosphere has been the subject of intensive investigation in recent years because of the need to assess the contribution of anthropogenically produced sulphur to acid rain, visibility reduction and climate modification.[1–4] Anthropogenic emissions of sulphur to the atmosphere are dominated by SO_2 whereas natural (biogenic) sulphur emissions are thought to be dominated by DMS derived from oceanic phytoplankton initiated by ultraviolet radiation from the sun.[5–8] At present, anthropogenic emissions of sulphur dominate; however, these emissions are predominantly in the northern hemisphere. In the southern hemisphere, and in particular from the southern oceans, natural emissions are extremely important. Typical day-time and night-time [DMS] levels in the troposphere are 120 and 50 pptv respectively.[8]

The main DMS oxidation reactions in the atmosphere are DMS + OH during the day and DMS + NO_3 at night. Subsequent oxidation leads to formation of species such as SO_2, H_2SO_4 and

[a] *Computational Chemistry Group, Department of Chemistry, Faculty of Science, University of Mauritius, Réduit 80837, Mauritius. E-mail: lyd.rhyman@gmail.com, p.ramasami@uom.ac.mu*
[b] *Centre For Natural Product Research, Department of Chemical Sciences, University of Johannesburg, Doornfontein, Johannesburg 2028, South Africa*
[c] *School of Chemistry and Chemical Engineering, University of Southampton, Highfield, Southampton SO17 1BJ, UK. E-mail: jmdyke@soton.ac.uk*

† Electronic supplementary information (ESI) available. See DOI: https://doi.org/10.1039/d5cp02065d

CH_3SO_3H (methane sulfonic acid or MSA). These species may contribute significantly to the acidity of the atmosphere and in the case of sulphuric acid to cloud formation. Molecular chlorine has been observed in coastal marine air. This is produced at night, as well as during the day, from heterogeneous reactions of ozone with wet sea-salt and is enhanced by the presence of ferric ions.[9–13] Night-time Cl_2 mixing ratios are higher than those during the day because of Cl_2 photolysis during the day. Comparison of recent experimentally measured Cl_2 concentrations in the lower atmosphere shows that typical day-time and night-time [Cl_2] levels are 5 and 50 pptv, respectively.[14–19] The DMS + Cl_2 reaction, which occurs mainly at night, provides another route for DMS loss and hence SO_2 production. This could contribute to explaining the discrepancy between known DMS decay rates and observed SO_2 production rates. Water is the third most abundant species in the troposphere behind only N_2 and O_2 with concentrations of up to 7.4×10^{17} molecules cm^{-3} (100% relative humidity; 0.03 atm.).[12] It has been demonstrated that water can change the rate coefficient of a reaction, by forming complexes with the reagents, products and transition states and lower their energies, and in this way, the activation barrier for a reaction may be reduced.[20–27]

We have previously studied the reaction of DMS with molecular chlorine (DMS + Cl_2) using UV photoelectron spectroscopy (PES), infrared matrix isolation spectroscopy and electronic structure calculations.[28–30] It was found that this reaction proceeds through the formation of a covalent reaction intermediate ($(CH_3)_2SCl_2$), in which sulphur is four coordinate. This then decomposes into the final products, monochlorodimethylsulphide (CH_3SCH_2Cl) and hydrogen chloride (HCl). Also, using PES as the detection technique, the room temperature rate coefficient of DMS + Cl_2 has been measured as $(3.4 \pm 0.7) \times 10^{-14}$ cm^3 $molecule^{-1}$ s^{-1},[28] four orders of magnitude lower than the DMS + Cl room temperature rate coefficient. One objective of our studies on DMS reactions of atmospheric importance is to investigate the effect of water on the reactions DMS + Cl and DMS + Cl_2 using electronic structure methods. The DMS + Cl reaction has recently been investigated in this way.[31] It was found that this reaction proceeds *via* four channels and, although water changes the mechanisms of these channels significantly, the presence of water was found not to affect the overall reaction rate coefficient under atmospheric conditions. Following on from this study, the aim of this present work is to study the reaction DMS + Cl_2 with and without water using electronic structure methods to establish the reaction energetics and mechanisms, and to determine if the energies of the transition states relative to the reagents are changed significantly when a single water molecule is present. In the earlier, mainly experimental studies,[28–30] a schematic potential energy diagram was constructed for the DMS + Cl_2 reaction. Minimum energy structures and transition states were located at the MP2/aug-cc-pVDZ level. In the present work, electronic structure calculations are performed at a higher level on the DMS + Cl_2 reaction in the absence and presence of a single water molecule to obtain improved relative energies, thermochemical values and structures of the energy minima and transition states.

2. Computational details

Electronic structure calculations were carried out to optimise the geometries of the reactants, reactant complexes, transition state structures (TSs), product complexes and products. As in our previous DMS + Cl work,[31] the M06-2X functional was used with aug-cc-pVTZ (aVTZ) basis set.[32] These computations were performed in the spin unrestricted formalism. The M06-2X functional was chosen because it has been shown to perform particularly well for TS structures and reaction barrier heights in benchmark studies on main group compounds.[33–37] Harmonic vibrational frequencies were calculated to verify the nature of the stationary points (minima and TSs), and to provide the zero-point energy (ZPE) and the thermodynamic contributions to the enthalpy and free energy changes. Intrinsic reaction coordinate (IRC) calculations were also performed to ensure that a given TS connects with the desired minima.[38,39]

Fixed point calculations were carried out using the UM06-2X/aVTZ optimised stationary point geometries, with the aug-cc-pVnZ basis sets (n = T and Q), using the domain-based local pair natural orbitals coupled cluster (DLPNO-UCCSD(T)) approach.[40–44] These were DLPNO-UCCSD(T)/aVnZ//UM06-2X/aVTZ (n = T and Q) calculations; the total energies obtained were extrapolated to the CBS limit employing the two parameter formula (eqn (2)):-[45,46]

$$E(x) = E_{CBS} + Ax^{-3} \quad (2)$$

where x = 3 (aVTZ) and 4 (aVQZ).

This DLPNO-CCSD(T) method employs localised orbitals and obtains the correlation energy as a sum over the correlation energies of electron pairs. It recovers a large part of the CCSD(T) correlation energy at low computational cost.

All DFT computations were carried out using Gaussian 16[47] running on SEAGrid.[48–51] The DLPNO-CCSD(T) single point calculations were performed using the ORCA package.[52,53]

3. Results and discussion

When one water molecule is added to DMS + Cl_2, the reaction could proceed in three ways depending on the initial (van der Waals) complex formed *i.e.* DMS + $Cl_2{\cdot}H_2O$, $DMS{\cdot}H_2O$ + Cl_2, $DMS{\cdot}Cl_2$ + H_2O. The computed minimum energy structures of the three van der Waals complexes $Cl_2{\cdot}H_2O$, $DMS{\cdot}H_2O$, $DMS{\cdot}Cl_2$ at the M06-2X/aVTZ level are shown in Fig. 1.

It was found that a common feature of the DMS + Cl_2 reaction with and without added water was that in each case the reaction can proceed along two pathways:- (i) the reactants to the covalently bound intermediate $(CH_3)_2SCl_2$ (H_2O) and on to the reaction products CH_3SCH_2Cl + HCl + (H_2O) and (ii) on a separate surface, the reactants to *cis*-CH_3SClCH_2:HCl (H_2O), and on to the products CH_3SCH_2Cl + HCl + (H_2O), where (H_2O) applies to the with-water case. The computed minimum energy

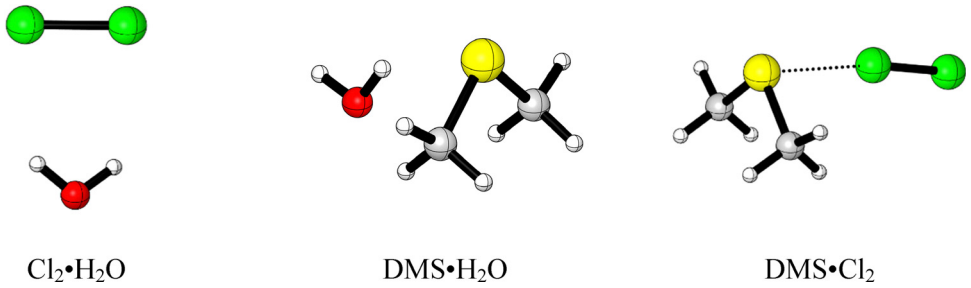

Fig. 1 Optimised minimum energy geometries of $Cl_2{\cdot}H_2O$, $DMS{\cdot}H_2O$ and $DMS{\cdot}Cl_2$.

structures of $(CH_3)_2SCl_2{\cdot}H_2O$ and *cis*-CH_3SClCH_2:$HCl{\cdot}H_2O$ at the M06-2X/aVTZ level are shown in Fig. 2.

The schematic potential energy diagram obtained at the DLPNO-CCSD(T)/CBS//M06-2X/aVTZ level for the DMS + Cl_2 reaction, in the absence of water, is shown in Fig. 3. The M06-2X/aVTZ and DLPNO-CCSD(T)/CBS//M06-2X/aVTZ relative electronic energies (ΔE, including zero-point energy (ZPE) corrections), relative enthalpies ($\Delta H^{\phi}_{f,298K}$) and relative free energies ($\Delta G^{\phi}_{f,298K}$) of the energy minima and transition states located are shown in Table 1. Comparison of the results shown in Fig. 3 with the results obtained in the earlier, mainly experimental work[28] at the MP2/aug-cc-pVDZ level (summarised in ref. 28) shows that the earlier results are incomplete with some stationary points not located, and the results are more approximate than the

Fig. 2 Optimised minimum energy geometries of $(CH_3)_2SCl_2{\cdot}H_2O$ and *cis*-CH_3SClCH_2:$HCl{\cdot}H_2O$.

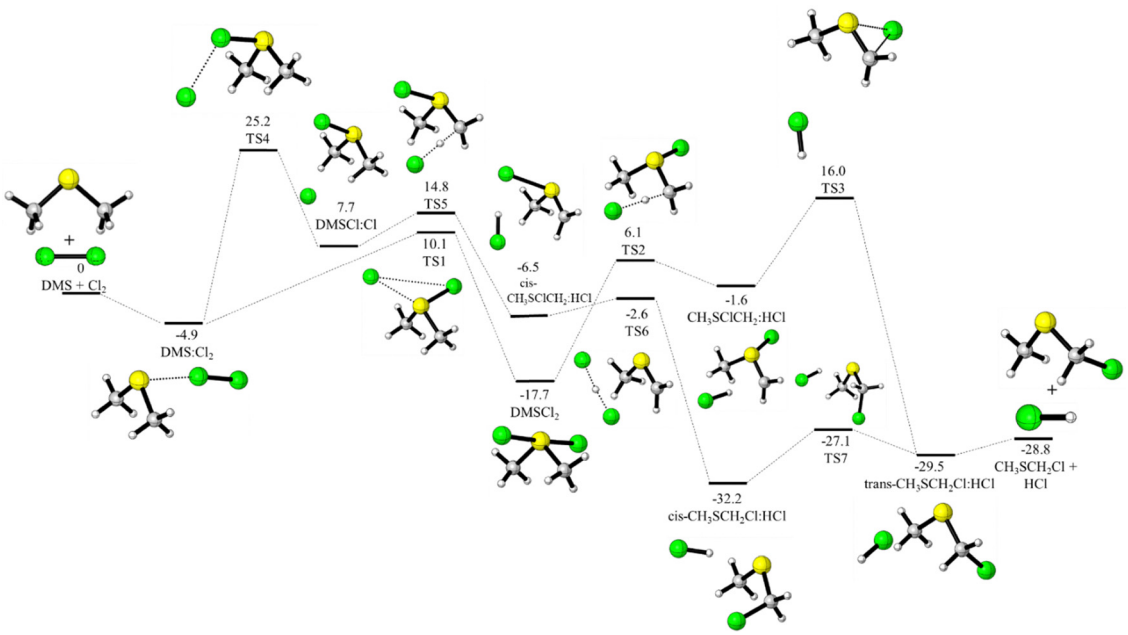

Fig. 3 Energy profile for the reaction of DMS + Cl_2 in the absence of water using the DLPNO-CCSD(T)/CBS//M06-2X/aVTZ method. DLPNO-CCSD(T)/CBS//M06-2X/aVTZ relative electronic energies (ΔE) including ZPE are shown in the figure.

Table 1 DMS + Cl_2 relative electronic energies (ΔE, kcal mol^{-1} incl. ZPE contributions), relative enthalpies (in brackets, $\Delta H^{\phi}_{f,298K}$ kcal mol^{-1})[a] and relative free energies (in italics, $\Delta G^{\phi}_{f,298K}$, kcal mol^{-1})

	M06-2X/aVTZ	DLPNO-CCSD(T)/CBS//M06-2X/aVTZ	MP2/aug-cc-pVDZ (ref. 28)
$DMS{\cdot}Cl_2$	−5.5 (−5.1) *2.3*	−4.9 (−4.6) *2.8*	−9.47
TS1	11.6 −10.8 *21.7*	10.1 −9.4 *20.3*	4.5
$DMSCl_2$	−16.3 (−16.5) *−7.1*	−17.7 (−17.9) *−8.5*	−26.29
TS2	6.5 (−5.9) *15.9*	6.1 (−5.5) *15.5*	2.75
CH_3SClCH_2:HCl	1.6 (−1.7) *9.7*	−1.6 (−1.4) *6.6*	Not located
TS3	18.9 (−19.4) *25.3*	16.0 (−16.6) *22.4*	8.35[b]
CH_3SCH_2Cl:HCl	−28.6 (−28.3) *−20.9*	−29.5 (−29.3) *−21.8*	−42.15
CH_3SCH_2 Cl + HCl	−27.6 (−27.3) *−27.3*	−28.8 (−28.4) *−28.5*	−32.06
TS4	26.1 (−25.6) *34.8*	25.2 (−24.7) *36.0*	Not located
DMSCl:Cl	9.1 (−8.8) *18.4*	7.7 (−7.4) *17.1*	2.43
TS5	14.7 (−14.1) *24.2*	14.8 (−14.3) *24.4*	(14.19 quoted in ref. 28) 11.38[b] (TS3 of ref. 28)
cis-CH_3SClCH_2:HCl	−3.9 (−3.8) *4.9*	−6.5 (−6.5) *2.2*	−14.69
TS6	−1.7 (−2.2) *7.3*	−2.6 (−3.0) *6.5*	−10.83 (TS4 of ref. 28)
cis-CH_3SCH_2Cl:HCl	−31.3 (−31.1) *−23.8*	−32.2 (−31.9) *−24.7*	−42.15
TS7	−26.5 (−26.9) *−17.8*	−27.1 (−27.6) *−18.5*	Not located

[a] The thermal correction to the enthalpy obtained using the M06-2X/aVTZ method were added to the DLPNO-CCSD(T) single point energy (ZPE is included in the electronic energies). [b] Not reported in the literature, we located the TS3 using the MP2/aVDZ method.

results presented here. In both cases pathways (i) and (ii) described above were identified. A summary of the relative energies of the common stationary points obtained in this work and in the lower level work of ref. 28 is given in Table 1. In this table, it can be seen that the present M06-2X/aVTZ and DLPNO-CCSD(T)/CBS results agree very well with each other, which supports their reliability, with the earlier lower-level MP2 energy values being mostly lower than the DLPNO-CCSD(T) values.

For formation of $(CH_3)_2SCl_2$ from the reactants, quoting the higher level DLPNO ΔE values (with the lower level ΔE values from ref. 28 shown in italics in brackets), the reactants first form a van der Waals complex $DMS{\cdot}Cl_2$ (at −4.9 (−9.5) kcal mol^{-1}) which converts *via* a transition state (TS1 at 10.1 (4.5) kcal mol^{-1}) to $(CH_3)_2SCl_2$ (at −17.7 (−26.3) kcal mol^{-1}). In comparison, *cis*-CH_3SClCH_2:HCl (at −6.5 (−14.7) kcal mol^{-1}) is formed from the van der Waals complex $DMS{\cdot}Cl_2$ *via* passage over a TS (TS4 at 25.2 kcal mol^{-1} (not located in ref. 28)) to give DMSCl:Cl (at +7.7 (2.4) kcal mol^{-1}) which converts *via* TS5 (at 14.8 (11.4) kcal mol^{-1}) to give *cis*-CH_3SClCH_2:HCl (see Fig. 3). The route from the covalently bound intermediate $(CH_3)_2SCl_2$ to the products is over TS2 (at 6.1 (2.7) kcal mol^{-1}) to CH_3SClCH_2:HCl (at −1.6 kcal mol^{-1}) (not located in ref. 28), and then over TS3 (at 16.0 (8.3) kcal mol^{-1}) to the product complex (*trans*-CH_3SCH_2Cl:HCl at −29.5 (−42.1) kcal mol^{-1}) and on to the products CH_3SCH_2Cl + HCl (at −28.8 (−32.0) kcal mol^{-1}). The route from the intermediate *cis*-CH_3SCH_2Cl:HCl to the products is *via* TS6 (at −2.6 (−10.8) kcal mol^{-1}) to *cis*-CH_3SCH_2Cl:HCl (at −32.2 (−42.1) kcal mol^{-1}) then *via* TS7 (at −27.1 kcal mol^{-1} (not located in ref. 28)) to the product complex *trans*-CH_3SCH_2Cl:HCl (at −29.5 (−42.1) kcal mol^{-1}) and on to the separate products CH_3SCH_2Cl + HCl (at −28.8 (−32.0) kcal mol^{-1}). As can be seen from Fig. 3, for the pathway *via* $(CH_3)_2SCl_2$, the highest barrier (rate determining) is TS3 (at 16.0 kcal mol^{-1}) whereas for the pathway *via cis*-CH_3SClCH_2:HCl the highest barrier is TS4 (at 25.2 kcal mol^{-1}).

The schematic reaction profiles of the DMS + Cl_2 reaction in the presence of one water molecule are shown in Fig. 4 and 5. Fig. 4 shows profiles which involve reaction *via* the hydrated covalently bound intermediate $(CH_3)_2SCl_2{\cdot}H_2O$ ($DMS{\cdot}H_2O{\cdot}Cl_2$ in Fig. 4) and Fig. 5 shows profiles which involve reaction *via* the hydrated intermediate *cis*-CH_3SClCH_2:HCl (CH_3SClCH_2:HCl-4 in Fig. 5). Overall, most of the minima and transition states seen in Fig. 3 (in the absence of water) for pathways (i) and (ii) have counterparts in Fig. 4 and 5, respectively (with water present).

As stated earlier, when one water molecule is added to DMS + Cl_2, the reaction could proceed *via* DMS + $Cl_2{\cdot}H_2O$, $DMS{\cdot}H_2O$ + Cl_2, $DMS{\cdot}Cl_2$ + H_2O. As shown in Fig. 4 and 5, the relative energies of these, relative to DMS + Cl_2 + H_2O, are DMS + $Cl_2{\cdot}H_2O$ (−0.5 kcal mol^{-1}) > $DMS{\cdot}H_2O$ + Cl_2 (−3.7 kcal mol^{-1}) > $DMS{\cdot}Cl_2$ + H_2O (−4.9 kcal mol^{-1}) (all values quoted are the higher level DLPNO ΔE values). DMS + $Cl_2{\cdot}H_2O$ and $DMS{\cdot}H_2O$ + Cl_2 correlate with a $DMS{\cdot}H_2O{:}Cl_2$ minimum at −8.5 kcal mol^{-1}, whereas $DMS{\cdot}Cl_2$ + H_2O correlates with another $DMS{\cdot}Cl_2{:}H_2O$ minimum at −9.4 kcal mol^{-1}. As shown in Fig. 4, both minima (at −8.5 and −9.4 kcal mol^{-1}) convert *via* TS1·H_2O (at +6.1 kcal mol^{-1})

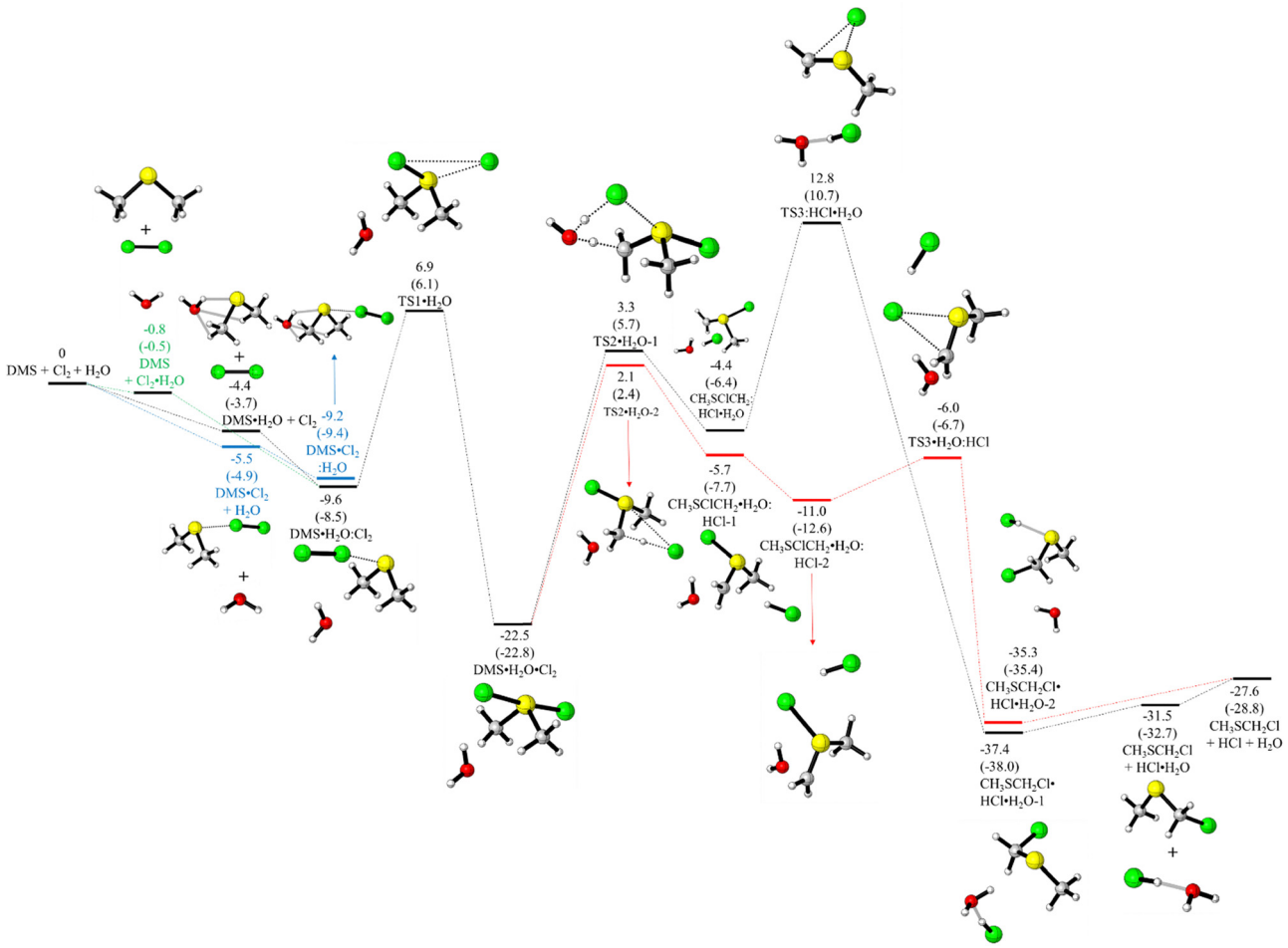

Fig. 4 Energy profiles for the reaction of DMS + Cl_2 + H_2O *via* the hydrated covalently bound intermediate $(CH_3)_2SCl_2{\cdot}H_2O$ using the M06-2X/aVTZ and DLPNO-CCSD(T)/CBS//M06-2X/aVTZ methods. The M06-2X/aVTZ relative electronic energies (ΔE) including ZPE are reported in the figure, with the DLPNO-CCSD(T)/CBS//M06-2X/aVTZ values shown in brackets; values are in kcal mol^{-1}. Note the DMS·Cl_2 complex (at −4.9 kcal mol^{-1}) connects with DMS·Cl_2·H_2O (at −9.4 kcal mol^{-1}) but this only correlates with TS4·H_2O-2 (20.1 kcal mol^{-1} in Fig. 5; DLPNO values quoted in brackets).

to the solvated covalently bound intermediate $(CH_3)_2SCl_2{\cdot}H_2O$ (at −22.8 kcal mol^{-1}). In contrast, on the *cis*-CH_3SClCH_2:HCl·H_2O pathway (Fig. 5), only the DMS·H_2O:Cl_2 minimum at −8.5 kcal mol^{-1} converts *via* TS4·H_2O-1 to a DMSCl·ClH_2O minimum energy structure at +2.3 kcal mol^{-1} which converts *via* TS5·H_2O-1 (at +4.7 kcal mol^{-1}) to a hydrated *cis*-CH_3SClCH_2·HCl minimum at −12.2 kcal mol^{-1} and the DMS·Cl_2:H_2O minimum at −9.4 kcal mol^{-1} converts *via* TS4·H_2O-2 (at +20.1 kcal mol^{-1}) to a DMSCl·H_2O:Cl structure at +2.9 kcal mol^{-1} which converts *via* TS5·H_2O-2 at 11.3 kcal mol^{-1} to CH_3SClCH_2:HCl·H_2O-3 at −12.0 kcal mol^{-1}. For the pathway *via* the intermediate $(CH_3)_2SCl_2$ in Fig. 3 each stationary point has an equivalent in Fig. 4. Significantly, taking the largest barriers in the no-water case, TS3 at +16.0 kcal mol^{-1} is lowered to TS3·H_2O:HCl at −6.7 kcal mol^{-1} (although there is a higher TS3 on a separate surface; TS3:HCl·H_2O at 10.7 kcal mol^{-1}). Similarly, the *cis*-CH_3SClCH_2:HCl pathway, TS4 (Fig. 3) is lowered from +25.2 kcal mol^{-1} to TS4·H_2O-1 at +6.3 kcal mol^{-1} (although there is a higher TS4 on a separate surface; TS4·H_2O-2 at +20.1 kcal mol^{-1}) and TS6 is lowered from −2.6 kcal mol^{-1} to TS6·H_2O-1 at −11.1 kcal mol^{-1} (Fig. 5). Also, it can be seen that TS6·H_2O-1 converts directly to a product complex ($CH_3SCH_2Cl{\cdot}HCl{\cdot}H_2O$-3 at −35.5 kcal mol^{-1}) (there is no TS7 to *trans*-CH_3SCH_2Cl:HCl as in the DMS + Cl_2 case with no water).

The computed relative electronic energies ΔE, as well as the relative ($\Delta H^{\phi}_{f,298K}$) and ($\Delta G^{\phi}_{f,298K}$) values, for the minima and transition states located in the with-water case are listed in Table 2.

As already described, the minimum energy geometries and formation energies (ΔE) relative to their reagents were computed for the van der Waals complexes DMS·H_2O, Cl_2·H_2O and DMS·Cl_2 at the UM06-2X/aVTZ and DLPNO-CCSD(T)/CBS//M06-2X/aVTZ levels. Also, the standard free energies ($\Delta G^{\phi}_{f,298K}$) and equilibrium constants (K_{eq}, 298 K) were computed for the formation of these complexes. This was done in order to determine the approximate relative concentrations of these complexes under typical tropospheric conditions. The computed ΔE, $\Delta G^{\phi}_{f,298K}$ and K_{eq} values are shown in Table 3 at the two levels of theory used. The following typical day-time/night-time concentrations of DMS, Cl_2 and H_2O were assumed, using values mentioned earlier.

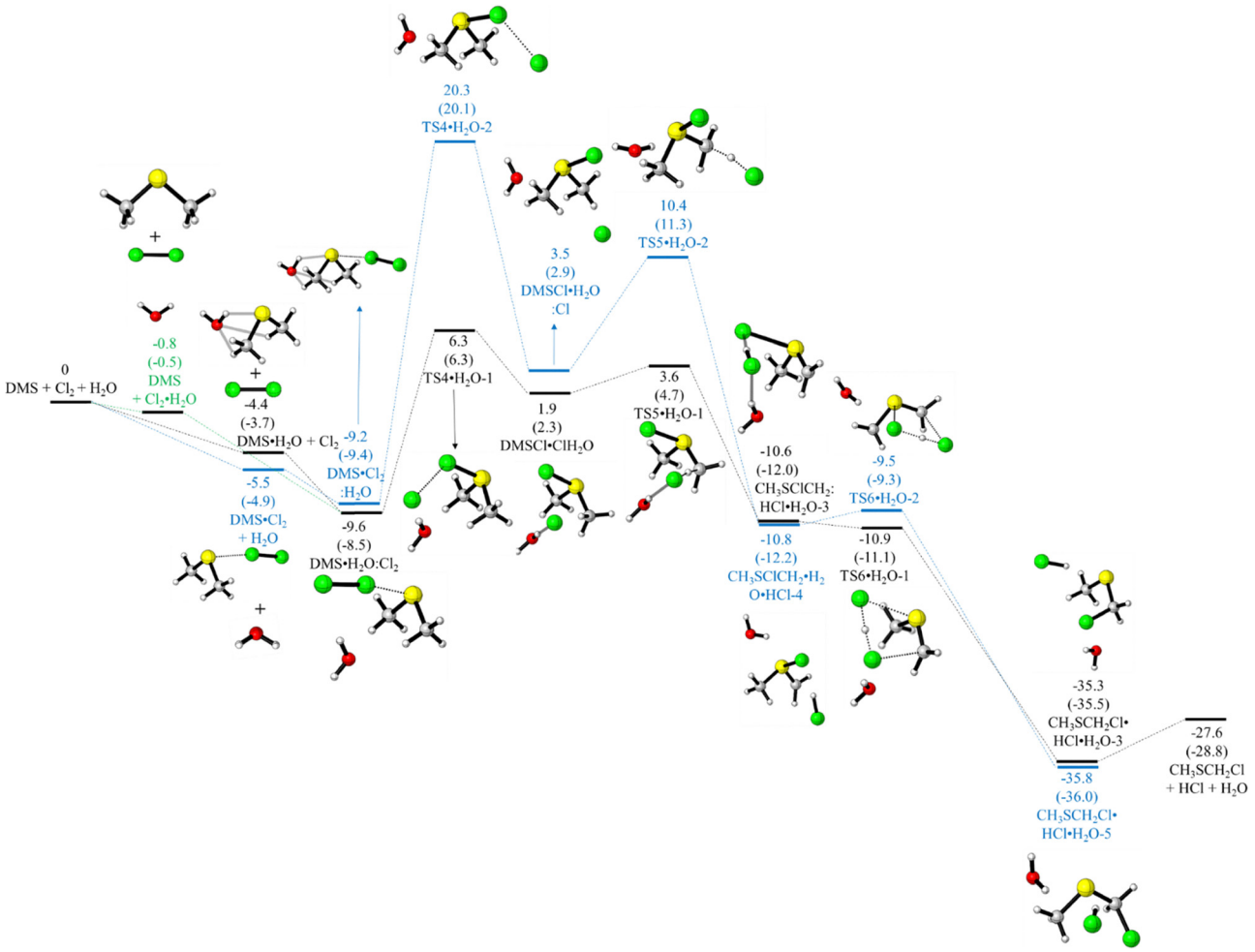

Fig. 5 Energy profiles for the reaction of DMS + Cl_2 + H_2O using the M06-2X/aVTZ and DLPNO-CCSD(T)/CBS//M06-2X/aVTZ methods *via* the hydrated intermediate *cis*-CH_3SClCH_2:HCl. The M06-2X/aVTZ relative electronic energies (ΔE) including ZPE are reported in the figure, with the DLPNO-CCSD(T)/CBS//M06-2X/aVTZ values shown in brackets; values are in kcal mol^{-1}.

[DMS] 120/50 ppt (2.95×10^9/1.23×10^9 molecules cm^{-3}), [Cl_2] 5/50 ppt (1.23×10^8/1.23×10^9 molecules cm^{-3}) and [H_2O] 7.38×10^{17}/7.38×10^{17} molecules cm^{-3} (ref. 8, 12, 14–19 and 31) With these estimated concentrations and the computed equilibrium constants for complex formation (Table 3), the estimated concentrations of the complexes at 298 K in the troposphere were in the order (Table 4) (a) [DMS·H_2O] > (b)[Cl_2·H_2O] ≫ (c) [DMS·Cl_2], with computed day-time/night-time values (in molecules cm^{-3}, at the DLPNO-CCSD(T)/CBS//M06-2X/aVTZ level) of [DMS·H_2O] =3.8×10^5/1.6×10^5, [Cl_2·H_2O] = 9.6×10^3/9.6×10^4, [DMS·Cl_2] = 1.3×10^{-4}/5.3×10^{-4} (see Table S2, ESI†).

Clearly, DMS·H_2O is the dominant complex under atmospheric conditions with Cl_2·H_2O slightly lower and DMS·Cl_2 much lower. [DMS·H_2O] and [Cl_2·H_2O] are comparable at night but [Cl_2·H_2O] is an order of magnitude lower than [DMS·H_2O] during the day. However, given that the estimated concentrations of DMS·H_2O and Cl_2·H_2O are much lower than the estimated concentrations of DMS, Cl_2 and H_2O, water will have only a minor effect on the overall rate coefficient under typical tropospheric conditions.

To demonstrate how these numbers were derived, the day-time [DMS·H_2O] is taken as an example. For the reaction

$$DMS + H_2O \rightarrow DMS \cdot H_2O \quad (3)$$

the equilibrium constant, K_{eq} at 298 K, has been calculated as 4.3×10^{-3} at the DLPNO-CCSD(T)/CBS//M06-2X/aVTZ level (see Table 3). Then

$$K_{eq} = [DMS \cdot H_2O]/P^{\phi}/(([DMS]/P^{\phi})\,[H_2O]/P^{\phi}) \quad (4)$$

$$= [DMS \cdot H_2O]P^{\phi}/([DMS] \cdot [H_2O]) \quad (5)$$

where P^{ϕ} is the standard pressure of 1 atmosphere (2.46×10^{19} molecues cm^{-3}).

Using the day-time values for [DMS] and [H_2O] listed in Table S1 (ESI†) (and quoted above), with K_{eq}= 4.3×10^{-3} gives [DMS·H_2O] = 3.80×10^5 molecules cm^{-3}.

As already stated, for formation of DMS·H_2O, Cl_2·H_2O and DMS·Cl_2 the computed K_{eq} ($\Delta G^{\phi}_{f,298K}$) values at the highest level (DLPNO-CCSD(T)/CBS) are 4.3×10^{-3} (3.22 kcal mol^{-1}), 2.6×10^{-3} (3.52 kcal mol^{-1}) and 8.7×10^{-3} (2.81 kcal mol^{-1}) (Table 3). These K_{eq} values need to be larger (*i.e.* the $\Delta G^{\phi}_{f,298K}$ values need to be more negative) in order for water to have any significant effect on the overall observed reaction rate. In order for the concentrations of DMS·H_2O and Cl_2·H_2O to be

Table 2 DMS + Cl_2 + H_2O Relative electronic energies (ΔE, kcal mol^{-1}, incl. ZPE contributions), relative enthalpies (in brackets, $\Delta H^{\phi}_{f,298K}$, kcal mol^{-1})[a] and relative free energies (in italic, $\Delta G^{\phi}_{f,298K}$, kcal mol^{-1})

	M06-2X/aVTZ	DLPNO-CCSD(T)/CBS//M06-2X/aVTZ
DMS·H_2O + Cl_2	−4.4 (−4.5) *2.5*	−3.7 (−3.8) *3.2*
DMS + Cl_2·H_2O	−0.8 (−0.5) *3.3*	−0.5 (−0.2) *3.5*
DMS·Cl_2 + H_2O	−5.5 (−5.1) *2.3*	−4.9 (−4.6) *2.8*
DMS·H_2O:Cl_2	−9.6 (−9.5) *6.9*	−8.5 (−8.4) *8.0*
DMS·Cl_2:H_2O	−9.2 (−8.8) *5.5*	−9.4 (−9.1) *5.2*
TS1·H_2O	6.9 (−6.2) *24.9*	6.1 (−5.4) *24.1*
DMS·H_2O·Cl_2	−22.5 (−22.9) *−5*	−22.8 (−23.2) *−5.3*
TS2·H_2O-1	3.3 (−1.7) *22.2*	5.7 (−4.1) *24.5*
CH_3SClCH_2:HCl·H_2O	−4.4 (−4.6) *12.2*	−6.4 (−6.6) *10.1*
TS3:HCl·H_2O	12.8 (−13.1) *27.9*	10.7 (−10.9) *25.7*
CH_3SCH_2Cl·HCl·H_2O-1	−37.4 (−37.6) *−23.2*	−38 (−38.3) *−23.8*
TS2·H_2O-2	2.1 (−1.5) *19.6*	2.4 (−1.8) *19.9*
CH_3SClCH_2·H_2O:HCl-1	−5.7 (−5.7) *10.6*	−7.7 (−7.7) *8.6*
CH_3SClCH_2·H_2O:HCl-2	−11.0 (−10.9) *5.6*	−12.6 (−12.6) *3.9*
TS3·H_2O:HCl	−6.0 (−6.8) *11.7*	−6.7 (−7.6) *10.9*
CH_3SCH_2Cl·HCl·H_2O-2	−35.3 (−35.1) *−19.9*	−35.4 (−35.2) *−20.0*
TS4·H_2O-1	6.3 (−5.0) *25.1*	6.3 (−5.0) *25.1*
DMSCl:Cl·H_2O	1.9 (−1.0) *19.9*	2.3 (−1.5) *20.4*
TS5·H_2O-1	3.6 (−2.8) *21.6*	4.7 (−3.8) *22.6*
CH_3SClCH_2:HCl·H_2O-3	−10.6 (−10.9) *6.4*	−12 (−12.3) *5*
TS6·H_2O-1	−10.9 (−11.8) *7.0*	−11.1 (−12.0) *6.8*
CH_3SCH_2Cl·HCl·H_2O-3	−35.3 (−35.1) *−20.0*	−35.5 (−35.3) *−20.2*
TS4·H_2O-2	20.3 (−19.9) *36.8*	20.1 (−19.7) *36.5*
DMSCl·H_2O:Cl	3.5 (−3.3) *20.5*	2.9 (−2.7) *19.9*
TS5·H_2O-2	10.4 (−10.0) *27.2*	11.3 (−10.9) *28*
CH_3SCH_2Cl·HCl·H_2O-4	−10.8 (−10.9) *6.2*	−12.2 (−12.3) *4.8*
TS6·H_2O-2	−9.5 (−10.2) *8.0*	−9.3 (−10.0) *8.2*
CH_3SCH_2Cl·HCl·H_2O-5	−35.8 (−35.5) *−21.2*	−36 (−35.7) *−21.4*
CH_3SCH_2Cl + HCl·H_2O	−31.5 (−31.7) *−25.6*	−32.7 (−32.9) *−26.7*
CH_3SCH_2Cl + HCl + H_2O	−27.6 (−27.3) *−27.3*	−28.8 (−28.4) *−28.5*

[a] The thermal correction to the enthalpy obtained using the M06-2X/aVTZ method were added to the DLPNO-CCSD(T) single point energy (ZPE is included in the electronic energies).

comparable with those of DMS and Cl_2, the DLPNO-CCSD(T)/CBS K_{eq} values for formation of these two complexes would have to increase by at least 3 orders of magnitude ($\Delta G^{\phi}_{f,298K}$ values for these complex formation reactions would have to decrease by ∼4.2 kcal mol^{-1} to ∼−1.0 kcal mol^{-1}). It is important to note that for these complexation reactions, ΔS is negative and hence $-T\Delta S$ makes a positive contribution to ΔG (in $\Delta G = \Delta H - T\Delta S$). Hence, a drop in temperature with altitude, as occurs in the troposphere up to ∼15 km at the

Table 3 Computed reaction energy (ΔE, kcal mol^{-1}) without ZPE correction, reaction free energy ($\Delta G_{298K}{}^{\phi}$, kcal mol^{-1}) and equilibrium constant (K_{eq}) at 298 K for formation of (a) DMS·H_2O, (b) Cl_2·H_2O and (c) DMS·Cl_2

	(a)	(a)	(a)	(b)	(b)	(b)	(c)	(c)	
	ΔE	$\Delta G_{298K}{}^{\phi}$	K_{eq}	ΔE	$\Delta G_{298K}{}^{\phi}$	K_{eq}	ΔE	$\Delta G_{298K}{}^{\phi}$	(c)
UM06/2X/aVTZ	−5.86	2.54	1.4×10^{-2}	−1.43	3.26	4.1×10^{-3}	−5.98	2.27	2.2×10^{-2}
DLPNO-CCSD(T)/CBS//M06-2X/aVTZ	−5.17	3.22	4.3×10^{-3}	−1.16	3.52	2.6×10^{-3}	−5.44	2.81	8.7×10^{-3}

Table 4 Estimated day-time and night-time concentration ratios of [DMS·H_2O], [Cl_2·H_2O] and [DMS·Cl] in the troposphere obtained using the appropriate K_{eq} values in Table 3 and estimated concentrations in Table S1 (ESI)

	UM06-2X/aVTZ	DLPNO-UCCSD(T)/CBS//UM06-2X/aVTZ	UM06-2X/aVTZ	DLPNO-UCCSD(T)/CBS//UM06-2X/aVTZ
	Day-time	Day-time	Night-time	Night-time
[DMS·H_2O]/[Cl_2·H_2O]	0.82×10^{2}	0.39×10^{2}	3.4	1.58
[DMS·H_2O]/[DMS·Cl_2]	3.8×10^{9}	2.9×10^{9}	3.8×10^{8}	2.9×10^{8}
[DMS·Cl_2]/[Cl_2·H_2O]	2.1×10^{-8}	1.3×10^{-8}	0.86×10^{-8}	0.58×10^{-8}

tropopause (typically from ∼298 to ∼220 K) will give rise to more negative values of ΔG. However, it can be seen from eqn (5) that [DMS·H_2O] depends on [H_2O]. Similarly [Cl_2·H_2O] depends on [H_2O]. Balloon-borne infrared emission measurements[54] show that water concentrations show a significant decrease with altitude being highest in the first 2 km of the atmosphere. At 3 km (typical temp. T_{typ} = 284 K) the [H_2O] values are approximately half of the 1 km (T_{typ} = 287 K) values and at 5 km (T_{typ} = 280 K) [H_2O] values are an order of magnitude lower than the 1 km value. Hence although the temperature drop with height would favour more negative ΔG values for the complexation reactions (a), (b) and (c) (and hence give larger K_{eq} values and larger complex concentrations), the large decrease of [H_2O] with height up to the tropopause, particularly in the first 5 km, is more significant and will dominate over the effect of a decrease in temperature, giving lower complex concentrations at heights greater than 2 km than those below 2 km. This is illustrated by the calculated values of [DMS·H_2O] at the altitudes of 0, 1, 3 and 5 km of 3.8×10^{5}, 2.4×10^{5}, 1.4×10^{5} and 0.25×10^{5} molecules cm^{-3} obtained with [H_2O] values at these altitudes from ref. 54 of 7.38×10^{17}, 3.49×10^{17}, 1.92×10^{17} and 0.31×10^{17} molecules cm^{-3} and computed DLPNO-CCSD(T)/CBS K_{eq} values at the temperatures at these altitudes of 4.3×10^{-3}, 5.9×10^{-3}, 6.3×10^{-3} and 6.9×10^{-3}.

As can be seen from Fig. 3–5, on including water in the DMS + Cl_2 reaction, the energy profiles are changed significantly. For example, for pathway (i) *via* the intermediate $(CH_3)_2SCl_2$, TS1 (10.1 kcal mol^{-1}) and TS3 (16.0 kcal mol^{-1}) are lowered significantly in the presence of water to TS1·H_2O (6.1 kcal mol^{-1}) and TS3·H_2O·HCl (−6.7 kcal mol^{-1}) respectively and there are two routes to the products from TS1·H_2O (6.1 kcal mol^{-1}) *via* TS3·H_2O:HCl (−6.7 kcal mol^{-1}) and *via* TS3:HCl·H_2O (10.7 kcal mol^{-1}). The highest barrier in pathway (i) in the lower energy route in the presence of water is TS1·H_2O (6.1 kcal mol^{-1}) compared to the highest barrier in the absence of water at TS1 (10.1 kcal mol^{-1}). For pathway (ii) *via* a *cis*-CH_3SClCH_2:HCl intermediate the very high barrier at TS4 without water (25.2 kcal mol^{-1}) is lowered to TS4·H_2O-1 (6.3 kcal mol^{-1}), which is the highest barrier for this pathway. This is comparable in energy to the highest barrier of the lower energy route for pathway (i), *via* TS1·H_2O (6.1 kcal mol^{-1}). Hence in the presence of water both pathways (i) and (ii) contribute to the overall reaction whereas the absence of water only pathway (i) *via* the intermediate $(CH_3)_2SCl_2$ contributes. (Cartesian coordinates for all stationary points located are summarised in Table S3, ESI†).

4. Conclusions

The present investigation of the DMS + Cl_2 reaction at the DLPNO-CCSD(T)/CBS//M06-2X/aVTZ level provides complete energy level diagrams for the reaction pathways which were not present in the earlier, lower-level MP2/aug-cc-pVDZ calculations. Potential energy diagrams computed for this reaction in the absence and presence of one water molecule at this higher level indicate that two pathways are present in both cases; they are (i) formation of the products CH_3SCH_2Cl + HCl + (H_2O) *via* a covalently bound intermediate $(CH_3)_2SCl_2$·(H_2O) and (ii) formation of the products *via* a *cis*-CH_3SClCH_2:HCl (H_2O) intermediate where (H_2O) applies to the with-water case. In general, the potential energy diagram is much more complex in the with-water case than in the no-water case and activation energy barriers are significantly reduced.

Three pathways were considered in the presence of water:-

$$DMS + Cl_2{\cdot}H_2O,\ DMS{\cdot}H_2O + Cl_2,\ DMS{\cdot}Cl_2 + H_2O$$

It was found that the reaction can proceed *via* all three pathways. However, as it is expected that [DMS·Cl_2] will be much lower than [DMS·H_2O] and [Cl_2·H_2O] in the atmosphere, reaction *via* DMS·Cl_2 + H_2O is likely to be insignificant. Also, as the estimated concentrations of Cl_2·H_2O, DMS·H_2O and DMS·Cl_2 are lower than those of DMS, H_2O and Cl_2 in the lower troposphere under typical atmospheric conditions, H_2O will have only a minor effect on the overall DMS + Cl_2 rate coefficient in the atmosphere.

It is expected that in the absence of water pathway (i) will be dominant whereas in the presence of water both pathways (i) and (ii) will contribute to the overall reaction.

Conflicts of interest

There are no conflicts to declare.

Data availability

Data supporting the results and findings of this work are included in the manuscript and ESI.†

Acknowledgements

This work used the Extreme Science and Engineering Discovery Environment (XSEDE), which is supported by National Science Foundation grant number OCI-1053575. LR and PR would also like to acknowledge computing facilities from the Centre for High Performance Computing of South Africa. LR also acknowledges the postdoctoral fellowship from the Higher Education Commission (formerly known as Tertiary Education Commission) of Mauritius.

References

1 R. J. Charlson, J. E. Lovelock, M. O. Andreae and S. G. Warren, *Nature*, 1987, **326**, 655–661.
2 S. F. Watts, *Atmos. Environ.*, 2000, **34**, 761–779.
3 T. S. Bates, B. K. Lamb, A. Guenther, J. Dignon and R. E. Stoiber, *J. Atmos. Chem.*, 1992, **14**, 315–337.
4 H. Berresheim, P. H. Wine and D. D. Davis, in *Composition, Chemistry and Climate of the Atmosphere*, ed R. Nostrand, New York, 1995, p. 251.
5 S. E. Schwarz, *Nature*, 1988, **336**, 441–445.
6 C. F. Cullis and M. M. Hirschler, *Atmos. Environ.*, 1980, **14**, 1263–1278.
7 T. S. Bates, J. D. Cline, R. H. Gammon and S. R. Kelly-Hansen, *J. Geophys. Res.*, 1987, **92**, 2930–2938.
8 A. Bandy, D. C. Thornton, B. W. Blomquist, S. Chen, T. P. Wade, J. C. Ianni, G. M. Mitchell and W. Nader, *Geophys. Lett.*, 1996, **23**, 741–744.
9 M. O. Andrea and P. J. Crutzen, *Science*, 1997, **276**, 1052–1058.
10 R. Vogt, P. J. Crutzen and R. Sander, *Nature*, 1996, **383**, 327–330.
11 B. J. Finlayson-Pitts, *Anal. Chem.*, 2010, **82**, 770–776.
12 B. Finlayson-Pitts and J. R. Pitts, *Chemistry of the Upper and Lower Atmosphere*, Academic Press, San Diego, CA, 2000.
13 J. D. Raff, B. Njegic, W. L. Chang, M. S. Gordon, D. Dabdub, B. Gerber and B. J. Finlayson-Pitts, *Proc. Natl. Acad. Sci. U. S. A.*, 2009, **106**, 13647–13654.
14 C. B. Faxon, J. K. Bean and L. H. Ruiz, *Atmosphere*, 2015, **6**, 1487–1506.
15 B. D. Finley and E. S. Saltzman, *Geophys. Res. Lett.*, 2006, **33**, L11809.
16 M. J. Lawler, B. D. Finley, W. C. Keene, A. A. P. Pszenny, K. A. Read, R. von Glasow and E. S. Saltzman, *Geophys. Res. Lett.*, 2009, **36**, L08810.
17 J. Liao, L. G. Huey, Z. Liu, D. J. Tanner, C. A. Cantrell, J. J. Orlando, F. M. Flocke, P. B. Shepson, A. J. Weinheimer, S. R. Hall, K. Ullmann, H. J. Beine, Y. Wang, E. D. Ingall, C. R. Stephens, R. S. Hornbrook, E. C. Apel, D. Riemer, A. Fried, R. L. Mauldin III, J. N. Smith, R. M. Staebler, J. A. Neuman and J. B. Nowak, *Nat. Geosci.*, 2014, **7**, 91–94.
18 T. P. Riedel, T. H. Bertram, T. A. Crisp, E. J. Williams, B. M. Lerner, A. Vlasenko, S. M. Li, J. Gilman, J. de Gouw, D. M. Bon, N. L. Wagner, S. S. Brown and J. A. Thornton, *Environ. Sci. Technol.*, 2012, **46**, 10463–10470.
19 C. W. Spicer, E. G. Chapman, B. J. Finlayson-Pitts, R. A. Plastridge, J. M. Hubbe, J. D. Fast and C. M. Berkowitz, *Nature*, 1998, **394**, 353–356.
20 R. J. Busek, J. S. Francisco and J. M. Anglada, *Int. Rev. Phys. Chem.*, 2011, **30**, 335–369.
21 V. Vaida, *J. Chem. Phys.*, 2011, **135**, 020901.
22 V. Vaida, H. G. Kjaergaard, P. E. Hulze and D. J. Donaldson, *Science*, 2003, **299**, 1566–1568.
23 V. Vaida, H. G. Kjaergaard and K. J. Feierabend, *Int. Rev. Phys. Chem.*, 2003, **22**, 203–219.
24 K. Morokuma and C. Muguruma, *J. Am. Chem. Soc.*, 1994, **116**, 10316–10317.
25 R. S. Zhu and M. C. Lin, *Chem. Phys. Lett.*, 2002, **354**, 217–226.
26 R. R. Li, J. R. A. Gorse, M. C. Sauer and S. Gordon, *J. Phys Chem*, 1980, **84**, 819–821.
27 M. A. Allodi, M. E. Dunn, J. Livada, K. N. Kirshner and G. C. Shields, *J. Phys. Chem. A*, 2006, **110**, 13283–13289.
28 J. M. Dyke, M. V. Ghosh, D. J. Kinnison, G. Levita, A. Morris and D. E. Shallcross, *Phys. Chem. Chem. Phys.*, 2005, **7**, 866–873.
29 J. M. Dyke, M. V. Ghosh, M. Goubet, E. P. F. Lee and G. Levita, *Chem. Phys.*, 2006, **324**, 85–95.
30 S. Beccaceci, J. S. Ogden and J. M. Dyke, *Phys. Chem. Chem. Phys.*, 2010, **12**, 2075–2082.
31 L. Rhyman, E. P. F. Lee, P. Ramasami and J. M. Dyke, *Phys. Chem. Chem. Phys.*, 2023, **25**, 4780–4793.
32 R. A. Kendall, T. H. Dunning Jr. and R. J. Harrison, *J. Chem. Phys.*, 1992, **96**, 6796–6806.
33 Y. Zhao and D. G. Truhlar, *Acc. Chem. Res.*, 2008, **41**, 157–167.
34 J. J. Zheng, Y. Zhao and D. G. Truhlar, *J. Chem. Theory Comput.*, 2009, **5**, 808–821.
35 L. Goerigk and S. Grimme, *Phys. Chem. Chem. Phys.*, 2011, **13**, 6670–6688.
36 X. F. Xu, I. M. Alecu and D. G. Truhlar, *J. Chem. Theory Comput.*, 2011, **7**, 1667–1676.
37 M. Bursch, J. M. Mewes, A. Hansen and S. E. Grimme, *Angew. Chem., Int. Ed.* 2022, **61**, e202205735.
38 C. Gonzalez and H. B. Schlegel, *J. Chem. Phys.*, 1989, **90**, 2154–2161.

39 C. Gonzalez and H. B. Schlegel, *J. Phys. Chem.*, 1990, **94**, 5523–5527.
40 C. Riplinger and F. Neese, *J. Chem. Phys.*, 2013, **138**, 034106.
41 C. Riplinger, B. Sandhoefer, A. Hansen and F. Neese, *J. Chem. Phys.*, 2013, **139**, 134101.
42 C. Riplinger, P. Pinski, U. Becker, E. F. Valeev and F. Neese, *J. Chem. Phys.*, 2016, **144**, 024109.
43 M. Saitow, U. Becker, C. Riplinger, E. F. Valeev and F. Neese, *J. Chem. Phys.*, 2017, **146**, 164105.
44 Y. Guo, C. Riplinger, U. Becker, D. G. Liakos, Y. Minenkov, L. Cavallo and F. Neese, *J. Chem. Phys.*, 2018, **148**, 011101.
45 T. Helgaker, W. Klopper, H. Koch and J. Noga, *J. Chem. Phys.*, 1997, **106**, 9639–9646.
46 A. Halkier, T. Helgaker, P. Jorgensen, W. Klopper, H. Koch, J. Olsen and A. K. Wilson, *Chem. Phys. Lett.*, 1998, **286**, 243–252.
47 M. J. Frisch, G. W. Trucks, H. B. Schlegel, G. E. Scuseria, M. A. Robb, J. R. Cheeseman, G. Scalmani, V. Barone, G. A. Petersson, H. Nakatsuji, X. Li, M. Caricato, A. V. Marenich, J. Bloino, B. G. Janesko, R. Gomperts, B. Mennucci, H. P. Hratchian, J. V. Ortiz, A. F. Izmaylov, J. L. Sonnenberg, D. Williams-Young, F. Ding, F. Lipparini, F. Egidi, J. Goings, B. Peng, A. Petrone, T. Henderson, D. Ranasinghe, V. G. Zakrzewski, J. Gao, N. Rega, G. Zheng, W. Liang, M. Hada, M. Ehara, K. Toyota, R. Fukuda, J. Hasegawa, M. Ishida, T. Nakajima, Y. Honda, O. Kitao, H. Nakai, T. Vreven, K. Throssell, J. A. Montgomery Jr., J. E. Peralta, F. Ogliaro, M. J. Bearpark, J. J. Heyd, E. N. Brothers, K. N. Kudin, V. N. Staroverov, T. A. Keith, R. Kobayashi, J. Normand, K. Raghavachari, A. P. Rendell, J. C. Burant, S. S. Iyengar, J. Tomasi, M. Cossi, J. M. Millam, M. Klene, C. Adamo, R. Cammi, J. W. Ochterski, R. L. Martin, K. Morokuma, O. Farkas, J. B. Foresman and D. J. Fox, *Gaussian16, Revision C.01*, Gaussian, Inc., Wallingford CT, 2016.
48 S. Pamidighantam, E. Nakandala, C. Abeysinghe, S. R. Wimalasena, S. Yodage, S. Marru and M. Pierce, *Int. Conf. Comput. Sci.*, 2016, **80**, 1927–1937.
49 N. Shen, Y. Fan and S. Pamidighantam, *J. Comput. Sci.*, 2014, **5**, 576–589.
50 R. Dooley, K. Milfeld, C. Guiang, S. Pamidighantam and G. Allen, *J. Grid. Comput.*, 2006, **4**, 195–208.
51 K. Milfeld, C. Guiang, S. Pamidighantam and J. Giuliani, *Proceedings of the 2005 Linux Clusters: The HPC Revolution*, Apr. 2005.
52 F. Neese, *Mol. Sci.*, 2012, **2**, 73–78.
53 F. Neese, F. Wennmohs, U. Becker and C. Riplinger, *J. Chem. Phys.*, 2020, **152**, 224108.
54 L. Palchetti, G. Bianchini, B. Carli, U. Cortesi and S. Del Bianco, *Atmos. Chem. Phys.*, 2008, **8**, 2885–2894.